# Liquid Crystalline Poly(ester amide)s Based on *N*,*N*′-Dimethyldiamines and an Aromatic Ester Triad

**T. F. McCarthy,† R. W. Lenz, and S. W. Kantor***

*Department of Polymer Science and Engineering, University of Massachusetts, Amherst, Massachusetts 01003*

**S. Curran**

*Corporate Technology, Allied-Signal Inc., Morristown, New Jersey 07960*

*Received March 20, 1996; Revised Manuscript Received March 11, 1997*[⊗]

ABSTRACT: A series of thermotropic liquid crystalline poly(ester amide)s was synthesized based on various *N*,*N*′-dimethylalkylenediamines and terephthaloyl bis(4-oxybenzoyl chloride), TBOC. Several different synthetic procedures were investigated to synthesize liquid crystalline (LC) polymers having a broad range of molecular weights. The highest molecular weight polymers were obtained by the low-temperature solution condensation of *N*,*N*′-bis(trimethylsilyl)diamines and TBOC. Analyses of the polymers by wide angle X-ray diffraction, differential scanning calorimetry, and polarizing optical microscopy showed that the as-prepared crystalline polymers melted to form a nematic, liquid crystalline phase, which showed no evidence of recrystallization upon cooling. The LC polyesteramides with a 6-methylene spacer unit exhibited a monotropic behavior in contrast to the polymers or copolymers with a 12-methylene spacer unit which are enantiotropic. Changes in polymer conformation which occurred on heating in the solid state and in the liquid crystalline state were evaluated by solid state $^{13}C$ cross polarization magic angle spinning NMR spectroscopy which showed that the polymers had considerable mobility at temperatures well below the crystalline melting point. The polymers, when precipitated from solution, contained mixtures of *syn* and *anti* amide units, but after melting, the *syn* amide unit was exclusively obtained indicating that it is likely the most thermodynamically stable conformation.

## Introduction

Few amide-containing thermotropic liquid crystalline polymers, TLCPs, have been synthesized to date,[1−10] so this study was directed at preparing amide-containing TLCPs capable of forming compatible blends with nylons. Blends containing both amorphous or semicrystalline polyamides have been shown to be immiscible with the TLCPs presently available, such as Hoechst-Celanese's Vectra.[11−14] Miscibility of such blends of TLCPs is not anticipated because of the inherent tendency of rigid-rod polymers to self-associate,[15] which makes the entropic energy of the blend even more unfavorable. Polyamides have only been shown to be compatible with either other polyamides or other polymers capable of highly specific interactions,[15−17] so rigid-rod polymers incorporating amide functional groups in the main chain would be expected to have better compatibility with various nylons.

Aromatic amide polymers generally have high melting temperatures, so for rodlike polyamides, a liquid crystalline phase generally cannot develop before polymer decomposition occurs. An object of this research was the design of an aromatic amide polymer having a melting temperature which allows formation of a liquid crystalline phase below the temperature of polymer degradation or isotropization. In order to synthesize amide-containing polymers having reduced melting points, the following strategies were employed: (1) hydrogen bonding was eliminated or reduced by incorporating *N*-methyl-substituted amide units into the polymer main chain; (2) aliphatic flexible spacer units were used to decouple the rigid-rod segments. By this approach, a series of main-chain nematic liquid crystalline poly(ester amide)s were synthesized based on terephthaloylbis(4-oxyphenylene carbonyl) units, which have been used previously to prepare many different liquid crystalline polyesters.[18−26] Several different *N*,*N*′-dimethylalkylenediamine monomers were used to synthesize the poly(ester amide)s.

Three different synthetic methods shown in Schemes 1 and 2 were evaluated for the preparation of the polymers with the objective of obtaining polymers having the highest possible molecular weights. Each method yielded polymers having the general chemical structure **X**.

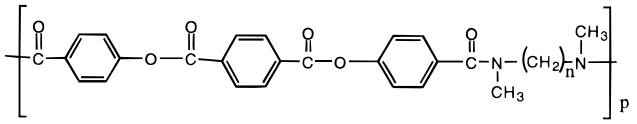

(**X**)

One objective of the present investigation was to determine the effect of *N*-methyl substituents on the physical properties of the resulting polymers. *N*-Methylated polyamides are well-known to yield polymers having lower melting transitions and significantly less crystallinity than analogous polyamides with unsubstituted amide units.[28−32] Many studies have shown that if the introduction of methyl or ethyl substituents into the flexible spacer units of liquid crystalline (LC) polyesters results in molecular asymmetry or dissymmetry, the crystal-to-liquid-crystal transition, the mesophase-to-mesophase transition, and the mesophase-to-isotropization transition temperatures are all lowered.[26,33−36] The introduction of these types of lateral substituents can also affect the ability of a liquid

† Current address: Polymer Research Center, Allied Signal Inc., Morristown, NJ 07962-1057.

[⊗] Abstract published in *Advance ACS Abstracts,* May 1, 1997.

S0024-9297(96)00421-4 CCC: $14.00 

crystalline polymer (LCP) to crystallize upon cooling from the molten state. In the present case the short *N*-methyl substituents used in this investigation are expected to yield polymers having reduced thermal transition temperatures but not necessarily reduced crystallinity, because substitution on both amide nitrogen atoms does not impart either asymmetry or dissymmetry to the repeating units.

Of particular interest in this investigation was the structure, conformation, and mobility of the TLCPs and the subsequent changes which occurred upon heating into the LC state. Because NMR chemical shifts are often sensitive to polymer conformation, high-resolution solid-state $^{13}$C-NMR has been successfully applied to the study of LCPs, both in the solid and in the molten states.[37−40] Solid-state $^{13}$C-NMR spectroscopy and wide-angle X-ray diffraction, WAXD, have been previously employed in the study of poly[tetramethyleneterephthaloyl bis(4-oxybenzoate)], a polymer very similar in structure to the polymers studied in this investigation. This polymer was shown to have two crystalline forms in the solid state, depending on the thermal history.[39]

One additional objective of this investigation was to study the existence and interconversion of *syn*- and *anti*-*N*-methylamide rotational isomeric states in the polymer main chain using solid-state $^{13}$C-NMR spectroscopy. Since the discovery of the hindered rotation of the amide linkage in dimethylformamide, numerous studies have been conducted investigating the *cis*-to-*trans* isomerization of the amide group for both small molecules and polymers.[41−43] The amide linkage of poly(*p*-phenyleneterephthalamide), PPTA, and other stiff amide-containing polymers were presumed to adopt the *trans* configuration from energy and steric considerations.[44] Extended polyamide chains having the *trans* conformation was recognized to be an important factor for the formation of the liquid crystalline state. Later Close et al. reported observing by solution NMR both the *cis* and *trans* conformations in dilute solutions.[45] This result was not confirmed by English using solid-state $^{13}$C-NMR where only the trans state was observed.[46] English asserted that in the study of Close, the PPTA was significantly degraded to oligomers during sample preparation, thus leading to the observations of *cis* and *trans* rotational conformers. *syn* and *anti* rotational conformers have been well characterized for *N*,*N*-dialkylamides but not extensively studied for polymers.[47] Investigation of the distribution of *syn* and *anti* rotational conformers was deemed important in the present study since a random distribution of *syn* and *anti* units might be expected to influence both the crystalline and the liquid crystalline states. Random sequences of *syn* and *anti* units would be expected to increase the intramolecular separation of the polymer chains and to retard the ability of the polymers to crystallize. Consequently, in order to fully characterize the polymers, the model compound *N*,*N*′-bis(benzoyl)-*N*,*N*′-dimethyl-1,4-butanediamine, M, was first synthesized and then studied.

Integral to this investigation was the characterization of the TLCPs by WAXD. With X-ray diffraction it should be possible to gain insight into the local molecular order of the TLCPs in both the solid and molten states, as well as the presence of molecular order between polymer chains.[48,49] The nematic state, for example, may consist of many small domains in which the parallel alignment of polymer chains persists over short distances, or it may have long range order where many polymer chains have a parallel alignment to form large nematic domains. The degree of long range order in a nematic LC phase will vary depending on polymer structure, temperature, and other factors. For example, highly oriented nematic domains can be obtained by magnetically aligning the polymer chains or by mechanical orientation obtained during fiber spinning. Because it was possible to synthesize polymers with high molecular weights in the present study, highly oriented fibers could be obtained from the liquid crystalline melt using a microextruder. The crystalline and liquid states were fully characterized by X-ray analysis using both powder and fiber samples at various temperatures.

## Experimental Section

All chemicals were obtained from the Aldrich Chemical Co. and used as received unless otherwise indicated. *p*-((Ethoxycarbonyl)oxy)benzoic acid and *p*-((ethoxycarbonyl)oxy)benzoyl chloride were prepared as described by Ober et al.[20] Methylene chloride, MC, was purified by successive washing with concentrated sulfuric acid, aqueous sodium carbonate, and water; predried with calcium chloride; and then distilled over $P_2O_5$. Triethylamine was predried with calcium sulfate and distilled from calcium hydride. Benzoyl chloride and chlorotrimethylsilane were distilled before use. Benzene was washed successively with concentrated sulfuric acid, water, and dilute aqueous sodium hydroxide; predried with calcium chloride; and distilled over lithium aluminum hydride. 1-Chloronaphthalene, 1-CN, was washed with aqueous sodium bicarbonate, dried with sodium sulfate, and then fractionally distilled at reduced pressure. Terephthaloyl chloride, TPCl, and isophthaloyl chloride, IPCl, were purified by sublimation. Chloroform was washed with water to remove ethanol, predried with calcium chloride, distilled from $P_2O_5$, and stored over 4 Å molecular sieves. Hexamethylphosphoramide, HMPA, was distilled from calcium hydride. 1-Methyl-2-pyrrolidinone, NMP, was purified by vacuum distillation. 1,1,2,2-Tetrachloroethane, TCE, was purified by successive washing with concentrated sulfuric acid, aqueous sodium carbonate, and water; predried with calcium chloride; fractionally distilled from $P_2O_5$; and stored over 4 Å molecular sieves.

**Monomer and Polymer Characterization.** Inherent viscosities for all polymers were determined at 29.5 °C either in trifluoroacetic acid or in TCE using a Cannon-Ubbelohde viscometer. Infrared spectra were obtained using a Perkin-Elmer 1600 Series Fourier transform infrared spectrophotometer. Varian XL-200 and XL-300 spectrometers were used to obtain carbon and proton spectra. The distortionless enhancement by polarization transfer spectra, DEPT, were obtained using a standard Varian package DEPT pulse sequence. Characterization of the poly(ester amide)s by polarizing optical microscopy, POM, was conducted using a Zeiss optical microscope equipped with a Mettler hot stage. Thermal analysis and thermal stability of the LCPs were measured on a Perkin-Elmer 7 series instrument equipped with a differential scanning calorimeter and a thermogravimetric analyzer under a stream of nitrogen at 10 °C/min. Peak maxima were used for the assignment of melting and cooling transition temperatures. The temperature and power ordinates of the DSC-7 were calibrated using an indium standard. Elemental analyses were conducted by the Microanalysis Laboratory of the University of Massachusetts at Amherst. Melting points were determined on a Fisher-Johns melting point apparatus and are uncorrected.

The X-ray diffraction patterns were obtained using point collimated Ni-filtered Cu Kα radiation from a Rigaku Denki X-ray generator with a Statton flat film camera. Two sample-to-film distances were employed, 49.64 and 168.78 mm, and were calibrated using calcium carbonate. The samples were placed in 1.5 mm Mark-Rohrchen glass capillaries within a copper heating cell. The dependence of X-ray intensity with $1/d$ (Å) was measured using an Optronics microdensitometer with a raster size of 50 $\mu$m.

Characterization of the molecular weights of polymers **IVB**, **IVC**, and **VIIIC** by gel permeation chromatography, GPC, was conducted using a Waters Model 6000A solvent delivery

system equipped with a R401 differential refractometer and two Jordi poly(divinylbenzene) columns: column 1 having a 1000 Å pore size and column 2 containing a mixed bed ($10^3$–$10^5$ Å). The GPC data were referenced to narrow molecular weight polystyrene obtained from Polysciences. The GPC traces were obtained in chloroform at a flow rate of 1.0 mL/min.

**Synthesis of Monomers and Model Compound M. *N,N′*-Bis(4-((ethoxycarbonyl)oxy)benzoyl)-*N,N′*-dimethyl-1,6-hexamethylenediamine, 1a.** To a flame-dried 250 mL three-neck round bottom flask equipped with an addition flask and a magnetic stirrer was added under nitrogen 5.0 g (0.035 mol) of *N,N′*-dimethyl-1,6-hexamethylenediamine, followed by the slow addition of 16.16 g (0.071 mol) of *p*-((ethoxycarbonyl)-oxy)benzoyl chloride in 50 mL of dry MC followed by an additional rinse with 70 mL of MC. The solution was stirred for 1 h at room temperature, after which 14.16 g (0.14 mol) of triethylamine was slowly added through the addition flask. The mixture was stirred overnight at room temperature and became light brown. Triethylamine hydrochloride was removed by filtration. To the filtrate was added 250 mL of diethyl ether. The solution was left overnight at 0 °C and subsequently filtered. The solution was evaporated to yield 16.0 g (88%) of a light brown liquid. Purification of **1a** was not necessary to obtain **2a** in good yields. The only impurity observed by thin layer chromatography was the starting material *p*-((ethoxycarbonyl)oxy)benzoyl chloride, which was used in slight excess. One gram of **1a** was purified by flash chromatography using a silica gel column which was 137 cm in length and 3 cm in diameter. *p*-((Ethoxycarbonyl)oxy)-benzoyl chloride was first eluted from the column using only acetonitrile as the elutant. **1a** was eluted from the column using a 5% methanol/95% acetonitrile solution. The fractions containing **1a** were combined, evaporated, and vacuum-dried at 60 °C for 1 day to yield **1a** as a clear liquid. The purer product may crystallize over a period of weeks at room temperature. Characterization of **1a** by IR spectroscopy showed the following absorptions (KBr): aromatic C−H stretch at 3075 $cm^{-1}$, aliphatic C−H stretches at 2962 and 2936 $cm^{-1}$, carbonate carbonyl stretch at 1767 $cm^{-1}$, and an amide carbonyl stretch at 1635 $cm^{-1}$.

***N,N′*Bis(4-hydroxybenzoyl)-*N,N′*-dimethyl-1,6-hexamethylenediamine, 2a.** To a solution containing 200 mL each of water and of ethanol was added 16.0 g (0.03 mol) of **1a** and 5.58 g (0.135 mol) of sodium hydroxide. The solution was refluxed for 1 h at 70 °C, cooled, and filtered to yield a pale yellow liquid. The ethanol was removed by rotary evaporation after which the aqueous solution was filtered to remove orange-colored impurities. To the aqueous solution was added glacial acetic acid which caused the immediate precipitation of a gummy solid mass. The mixture was refluxed and cooled to 0 °C, and the precipitate was collected by filtration and washed with copious amounts of water. The crude product was recrystallized from 30% aqueous ethanol (1 g/100 mL), filtered, and washed with cold ethanol to yield 7.38 g (64% yield) of **2a**. Characterization of **2a** by IR spectroscopy showed the following absorptions (KBr): broad O−H stretch at 3189 $cm^{-1}$, aliphatic C−H stretches at 2932 and 2855 $cm^{-1}$, amide carbonyl stretch at 1607 $cm^{-1}$, and a ring carbon−carbon stretch at 1602 $cm^{-1}$.

***N,N′*-Bis(trimethylsilyl)-*N,N′*-dimethyl-1,12-dodecamethylenediamine, 3c.** A silyl-substitued diamine having 12 methylene units will be described for illustrative purposes. *N,N′*-Dimethyl-1,12-dodecamethylenediamine (52.37g, 0.229 mol), prepared according to the method of Devinsky,[50] was placed in an oven-dried reaction vessel consisting of a 1000 mL three-neck round-bottom flask equipped with a large magnetic stirrer, a reflux condenser, and an addition funnel. All manipulations were carried out under an argon atmosphere. To the flask was added 600 mL of dry benzene, followed by the slow addition of chlorotrimethylsilane (66.68 mL, 0.525 mol), after which the reaction vessel was heated at reflux for 90 min. The reaction vessel was cooled to room temperature, triethylamine (97.4 mL, 0.70 mol) was added, and the reaction was refluxed for one additional day. Triethylamine hydrochloride readily precipitated from the reaction mixture. The mixture was allowed to cool to room temperature, and then filtered under argon pressure. The triethylamine hydrochloride residue was washed with 400 mL of dry benzene. The desired product was distilled at 145 °C under 0.9 mm of mercury to obtain **3c** in 81% yield. Characterization of the neat *N,N′*-trimethylsilyl-*N,N′*-dimethylalkylenediamines by IR showed the following vibrations: 2929 $cm^{-1}$, 2854 $cm^{-1}$ (C−H stretching); 1248 $cm^{-1}$ (Si−$CH_3$ symmetric deformation); 834 $cm^{-1}$ (Si−C stretching and methyl rocking).

***N,N′*-Bis(benzoyl)-*N,N′*-dimethyl-1,4-butanediamine, Model Compound M.** The synthesis of compound **M** has been reported previously from *N,N′*-dimethyl-1,4-butanediamine and benzoyl chloride.[51] Model compound **M** (**4a**) had the following IR absorptions (KBr): aromatic C−H stretch at 3060 $cm^{-1}$, 3009 $cm^{-1}$, aliphatic C−H stretches at 2928 and 2866 $cm^{-1}$, an amide carbonyl stretch at 1625 $cm^{-1}$, and a ring carbon−carbon stretch at 1600 $cm^{-1}$.

**Polymer Syntheses. Poly[(methylamino)hexamethylene(methylamino)carbonyl-*p*-phenyleneoxycarbonyl-*p*-phenylenecarbonyloxy-*p*-phenylenecarbonyl], IA.** This polymer was obtained from **2a** and terephthaloyl chloride. To an oven-dried flask equipped with a reflux condenser and an argon inlet was added 2.0 g (5.2 mmol) of **2a** and 1.056 g (5.2 mmol) of terephthaloyl chloride, followed by 40 mL of dry 1-CN. The reaction vessel was heated at 240 °C for 2 days under argon and then cooled, and the polymer was precipitated in methanol, filtered, extracted in a Soxhlet with methanol for 1 day, and vacuum-dried for 2 days at 50 °C to yield 1.89 g of polymer, **IA**.

**Poly[(methylamino)dodecamethylene(methylamino)-carbonyl-*p*-phenylene-oxycarbonyl-*p*-phenylenecarbonyloxy-*p*-phenylenecarbonyl], IB.** A solution of 0.88 g (3.8 mmol) of *N,N′*-dimethyldodecamethylenediamine in 100 mL of dry chloroform and a solution of 1.71 g (3.8 mmol) of terephthaloyl bis(4-oxybenzoyl chloride), TBOC,[23] in 200 mL of dry chloroform were added simultaneously to a Waring blender containing 0.426 g (7.6 mmol) of potassium hydroxide dissolved in 200 mL of distilled water. The resulting mixture was mixed at high speed under a nitrogen purge for 40 min. The product was precipitated in methanol, filtered, extracted in a Soxhlet for 1 day with methanol, and vacuum-dried to yield 0.95 g of polymer, **IB**.

**Poly[(methylamino)octamethylene(methylamino)-carbonyl-*p*-phenyleneoxycarbonyl-*p*-phenylenecarbonyloxy-*p*-phenylenecarbonyl], VIIB.** A 0.47 g (2.73 mmol) portion of *N,N′*-dimethyloctamethylenediamine was added to 5.45 mL of 1 N HCl to yield a clear solution. This solution was further diluted with 70 mL of distilled water. An equimolar amount of TBOC (1.22 g, 2.73 mmol) was dissolved in 200 mL of chloroform. A solution of 0.673 g of potassium hydroxide in 100 mL of distilled water was first added to a Waring blender, followed by the simultaneous addition of the diamine and diacid chloride solutions. The reaction mixture was stirred at high speed in the Waring blender for 1 h under an argon purge. The polymer was precipitated in methanol, collected by filtration, extracted in a Soxhlet with methanol for 1 day, and then vacuum-dried for 1 day to yield 0.57 g of polymer, **VIIB**.

**Poly[(methylamino)hexamethylene(methylamino)-carbonyl-*p*-phenyleneoxycarbonyl-*p*-phenylenecarbonyloxy-*p*-phenylenecarbonyl], VIIC.** All manipulations were carried out in thoroughly dried glassware because of the sensitivity of the disilamines to moisture. A 500 mL three-neck round-bottom flask was equipped with a magnetic stirrer and an addition flask. The disilyl derivative **3a** (20.125 g, 69.7 mmol) was weighed into the addition flask under argon. An equimolar amount (30.90 g, 69.7 mmol) of TBOC was added to the round-bottom flask under nitrogen. Two hundred milliliters of dry TCE was added to the diacid chloride solid to yield a mixture which was cooled to −30 °C. The silyl-substituted monomer, **3a**, was slowly added to the round-bottom flask through the addition funnel. The reaction was stirred between −10 and −30 °C for 4 h. The acid chloride gradually dissolved in the TCE solution as it reacted to form polymer. After 4 hours the solution was allowed to warm to

**Scheme 1**

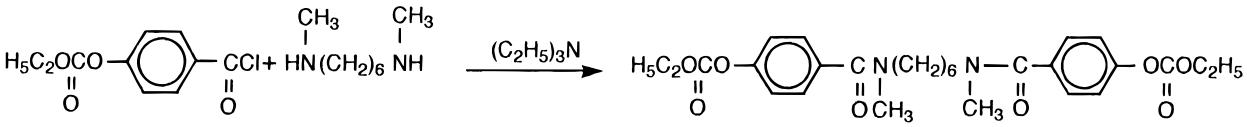

**1a**

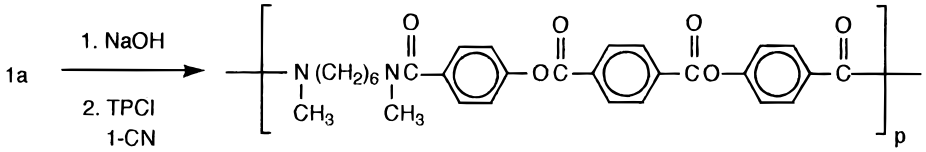

**IA**

**Table 1. Yields, Melting Points, and Elemental Analyses of Derivatives of *N,N′*-Dimethylalkylenediamines**

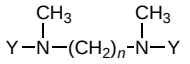

| compound | *n* | Y | % yield | mp, °C | bp, °C | formula | | C | H | N |
|---|---|---|---|---|---|---|---|---|---|---|
| **1a** | 6 | $C_2H_5OCO_2PhCO-$[a] | 88 | 54−55 | | $C_{28}H_{36}O_8N_2$ | calcd | 63.62 | 6.87 | 5.30 |
| | | | | | | | found | 63.32 | 6.90 | 5.47 |
| **2a** | 6 | HOPhCO−[a] | 64 | 209−211 | | $C_{22}H_{28}O_4N_2$ | calcd | 68.72 | 7.34 | 7.28 |
| | | | | | | | found | 68.55 | 7.30 | 7.22 |
| **3a** | 6 | $(CH_3)_3Si-$ | 86 | | 63/0.13[b] | $C_{14}H_{36}N_2Si_2$ | calcd | 58.26 | 12.57 | 9.96 |
| | | | | | | | found | 58.07 | 12.44 | 9.96 |
| **3b** | 8 | $(CH_3)_3Si-$ | 66 | | 103/0.9[b] | $C_{16}H_{40}N_2Si_2$ | calcd | 60.68 | 12.73 | 8.85 |
| | | | | | | | found | 60.40 | 12.49 | 9.04 |
| **3c** | 12 | $(CH_3)_3Si-$ | 81 | | 145/0.9[b] | $C_{18}H_{48}N_2Si_2$ | calcd | 64.44 | 12.98 | 7.52 |
| | | | | | | | found | 64.33 | 12.84 | 7.65 |
| **M** | 4 | PhCO− | 66 | 117−118 | | $C_{20}H_{24}O_2N_2$ | calcd | 74.04 | 7.46 | 8.64 |
| | | | | | | | found | 73.84 | 7.49 | 8.60 |

[a] Para substituted. [b] Torr.

room temperature. The reaction was stirred for 2 days at room temperature to yield a viscous solution. The solution was poured in methanol to yield a fibrous polymer, which was filtered, extracted in a Soxhlet with methanol for 1 day, and vacuum-dried to yield 35.3 g of polymer **VIIC**.

**X-ray Diffraction Studies.** Polymer fiber from polymer **VIIIC** was prepared by compression molding the neat polymer powder at 275 °C for 6 min under vacuum. Subsequently, it was ground into a fine powder, vacuum-dried for an additional day, melt-extruded through a Randcastle Microtruder where the maximum temperature was 271 °C, and collected as a continuous filament at a pickup speed of 115 m/min. Poly(ester amide) fiber obtained from polymer **VIIIC** will be denoted as **PEA-VIIIC**. Samples of the fiber were placed in glass capillaries and exposed to X-rays successively for 4 h at the following temperatures: room temperature, 138, 180, 218, and 238 °C. A separate investigation was employed using a longer sample-to-film distance (168.78 mm) in order to better characterize the X-ray reflections occurring at lower angles. These fibers were exposed for at least 24 h at the following temperatures room temperature, 120, 180, and 213 °C.

Polymer **VIIC** was also compression molded, ground into a fine powder, and melt-extruded through the Randcastle Microtruder where the maximum temperature was 300 °C. A continuous filament was stretched from the melt by hand. The fiber obtained from polymer **VIIC** will be designated **PEA-VIIC**.

Polymer **IVB** was investigated by X-ray diffraction as a powder. A sample was exposed successively for 2.5 h at room temperature, 2.5 h at 175 °C, and 4.0 h 250 °C. Another sample of **IVB** was sealed in a glass capillary and heated on a Fisher-Johns melting point apparatus for 6 min at 280 °C to ensure complete melting of the polymer. The sample was then cooled at a rate of approximately 10 °C/min to room temperature. The cooled sample was then exposed to X-rays at room temperature and will be designated **PEA-IVB**.

## Results and Discussion

**Monomer and Polymer Preparation.** With the objective of preparing high molecular weight LC polymers having the general structure **X** shown in the Introduction, three preparative methods were employed using known synthetic methods for amides. The first synthetic route used is shown in Scheme 1. This method involved the use of a series of blocking and deblocking steps.[20] *p*-((Ethoxycarbonyl)oxy)benzoic acid was first prepared from *p*-hydroxybenzoic acid and ethyl chloroformate and converted to *p*-((ethoxycarbonyl)oxy)-benzoyl chloride by reaction with thionyl chloride according to the literature preparation.[13] Scheme 1 yielded the intermediate **1a** and monomer **2a** in reasonable yields, in spite of the difficult purification of **1a** because of its reluctance to crystallize. However, **2a** could be synthesized in reasonable yield and purified without the intermediate purification of **1a**. The physical properties, elemental analyses, and $^1$H-NMR peak assignments for **1a**, **2a**, and **4a** are given in Tables 1 and 2.

The polymers prepared according to Scheme 1 had the lowest solution viscosities, which might be attributed to the lack of solubility of **2a** in nonpolar reaction solvents, such as 1-chloronaphthalene. Significant degradation occurred at the temperatures necessary to solubilize the diphenol, **2a**. Scheme 2 is used for polymer preparations.

Polymers **I**−**VIIB** were prepared by the second synthetic method using the direct condensation of tereph-

**Table 2. $^1$H-NMR Chemical Shifts ($\delta$) of Derivatives of *N,N′*-Dimethylalkylenediamines[a]**

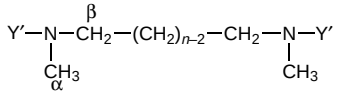

| Compound | n | Temp. | Y′ | α (s) | β [1] | Other $^1$H |
|---|---|---|---|---|---|---|
| **1a**[2] | 6 | RT | 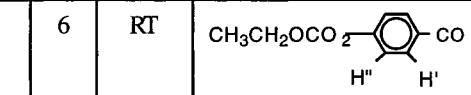 | 3.01<br>2.92 | 3.46<br>3.20 | $CH_3CH_2O$ 4.29 (q); $CH_3CH_2O$ 1.37 (t);<br>H′ 7.39 (d); H″ 7.21 (d);<br>N-$CH_2(CH_2)_{n-2}CH_2$-N 0.95-1.73 (m) |
| **1a**[3] | 6 | 80°C | 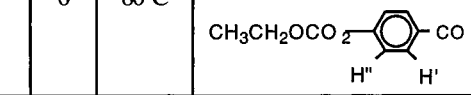 | 2.96 | 3.30 | $CH_3CH_2O$ 4.29 (q); $CH_3CH_2O$ 1.37 (t);<br>H′ 7.44 (d); H″ 7.27 (d);<br>N-$CH_2(CH_2)_{n-2}CH_2$-N 1.28-1.58 (m) |
| **2a**[4] | 6 | RT | 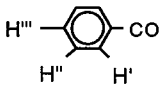 | 3.00 | 3.38 | HO 4.92 (s); H′ 7.26 (broad singlet);<br>H″ 6.84 (d);<br>N-$CH_2(CH_2)_{n-2}CH_2$-N 1.45-1.90 (m) |
| **3a**[5] | 6 | RT | $(CH_3)_3Si$- | 2.43 | 2.72 | $(CH_3)_3Si$ 0.12 (s); N-$CH_2CH_2$ 1.47 (m)<br>N-$CH_2CH_2(CH_2)_{n-4}CH_2CH_2$-N 1.28 (m) |
| **3b**[5] | 8 | RT | $(CH_3)_3Si$- | 2.49 | 2.68 | $(CH_3)_3Si$ 0.14 (s); N-$CH_2CH_2$ 1.47 (m)<br>N-$CH_2CH_2(CH_2)_{n-4}CH_2CH_2$-N 1.35 (m) |
| **3c**[2] | 12 | RT | $(CH_3)_3Si$- | 2.45 | 2.74 | $(CH_3)_3Si$ 0.05 (s); N-$CH_2CH_2$ 1.47 (m)<br>N-$CH_2CH_2(CH_2)_{n-4}CH_2CH_2$-N 1.30 (m) |
| **M**[2] | 4 | RT | 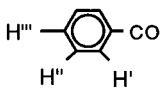 | 3.09<br>2.95<br>2.87 | 3.61<br>3.43<br>3.30 | H′ 7.39 (s); H″ 7.39 (s); H‴ 7.39 (s) |
| **M**[3] | 4 | 80°C | 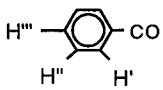 | 2.90 | 3.33 | H′ 7.44 (s); H″ 7.36 (s); H‴ 7.44 (s) |

[a] Key: 1, broad peak which appears as a singlet for **1a** and M at 80 °C; 2, in $CDCl_3$; 3, in DMSO-$d_6$. 4, in $CD_3OD$; 5, in pyridine-$d_6$.

**Scheme 2**

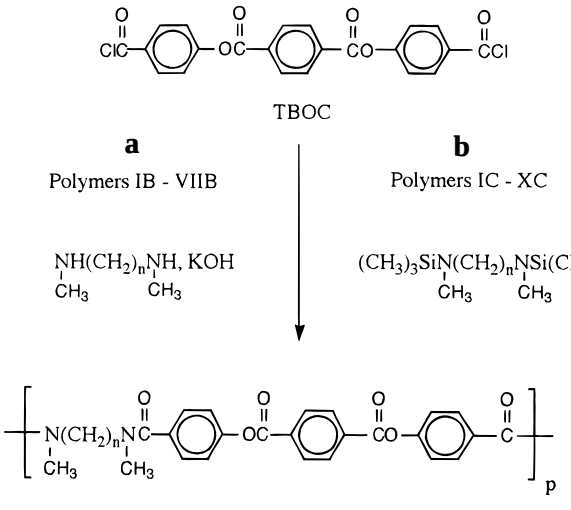


thaloyl bis(4-oxybenzoyl chloride), TBOC, with a *N,N′*-dimethylalkylenediamine using an acid acceptor, as shown in Scheme 2a. TBOC was prepared by the condensation of *p*-hydroxybenzoic acid with terephthaloyl chloride yielding terephthaloyl bis(4-oxybenzoic acid), which was readily converted to the corresponding acid chloride by reaction with thionyl chloride.[22] This preparation involved fewer synthetic steps because the mesogenic unit was prepared without a series of protection and deprotection steps.

Polymers prepared according to Scheme 2a had inherent viscosities between 0.3 and 0.4 dL/g. Because the *N,N′*-dimethylalkylenediamines had limited solubility in water, the polymers were prepared by dissolving TBOC and the appropriate *N*-methylated diamine in separate solutions of chloroform followed by rapid mixing. The polymerization was conducted in a Waring blender using a basic aqueous phase to neutralize the HCl liberated during the polymerization reaction. The deficiency of this synthetic method was the poor solubility of TBOC in common solvents. For example, TBOC has a solubility in chloroform at reflux of approximately 1 g per 100 mL. Consequently, the polymerization reactions were conducted at very dilute concentrations. Polymer **VIIB** was prepared by adding the hydrochloride salt of *N,N′*-dimethyl-1,8-octamethylenediamine dissolved in an aqueous phase to TBOC dissolved in an organic phase, but this interfacial type of polymerization reaction yielded polymers in only low yields and with low inherent viscosities.

The highest molecular weight poly(ester amide)s, polymers **IC**−**XC**, were prepared by the direct condensation of TBOC with trimethylsilyl-substituted *N,N′*-dimethylalkylenediamines, as shown in Scheme 2b, without the need for an added base. Polymers obtained

**Table 3. Reaction Conditions, Yields, and Solution Viscosities of the Poly(ester amide)s**

| polymer | *n* | temp (°C) | base | solvent | yield (%) | $\eta_{inh.}$[a] |
|---|---|---|---|---|---|---|
| **IA**[b] | 6 | 270 | | 1-chloronaphthalene | 71 | 0.09 |
| **IIA**[b] | 6 | 240 | | 1-chloronaphthalene | 60 | 0.13 |
| **IB** | 12 | RT[d] | KOH | chloroform | 42 | 0.36 |
| **IIB** | 10 | RT | KOH | chloroform | 64 | 0.38 |
| **IIIB** | 75% 12, 25% 6[c] | RT | KOH | chloroform | 64 | 0.39 |
| **IVB** | 50% 12, 50% 6[c] | RT | KOH | chloroform | 56 | 0.38 |
| **VB** | 25% 12, 75% 6[c] | RT | KOH | chloroform | 46 | 0.34 |
| **VIB** | 6 | RT | KOH | chloroform | 39 | 0.31 |
| **VIIB** | 8 | RT | KOH | chloroform/$H_2O$ | 40 | 0.24 |
| **IC** | 8 | 100 | | HMPA/NMP | 28 | 0.25 |
| **IIC** | 8 | RT to 70 | | chloroform | 76 | 0.35 |
| **IIIC** | 8 | RT to 100 | | NMP | 65 | 0.49 |
| **IVC** | 8 | RT to 150 | | tetrachloroethane | 81 | 0.54 |
| **VC** | 6 | RT to 150 | | tetrachloroethane | 78 | 0.45 |
| **VIC** | 6 | RT to 150 | | tetrachloroethane | 79 | 0.53 |
| **VIIC** | 6 | −10 to −30 | | tetrachloroethane | 99 | 0.84 (0.38) |
| **VIIIC** | 46% 12, 54% 6[c] | −10 to −30 | | tetrachloroethane | 98 | 1.23 |
| **IXC** | 46% 12, 54% 6[c] | −10 to −30 | | tetrachloroethane | 96 | 1.61 (1.00) |
| **XC** | 6 | −10 to −70 | | tetrachloroethane | 95 | (0.88)[e] |

[a] Trifluoroacetic acid or (TCE), 0.5 g/dL. [b] The internal aromatic group was a terephthaloyl unit for **IA** and an isophthaloyl unit for **IIA**. [c] Mole %. [d] Room temperature. [e] **XC** was insoluble in TFA forming an oily emulsion.

**Table 4. Molecular Weights of Polymers Characterized by GPC and Elemental Analyses**

| | | | | | calculated, % | | | found, % | | |
|---|---|---|---|---|---|---|---|---|---|---|
| polymer | $M_n$ | $M_w$ | PDI[a] | $DP_n$[b] | C | H | N | C | H | N |
| **IVB** | 5 598 | 7 892 | 1.32 | 10 | 71.20 | 6.52 | 5.03 | 70.23 | 6.25 | 4.58 |
| **IVC** | 29 027 | 46 056 | 1.59 | 54 | 70.83 | 6.32 | 5.16 | 70.05 | 6.30 | 5.l0 |
| **VIIIC** | 48 900 | 68 011 | 1.39 | 88 | 71.10 | 6.47 | 5.06 | 70.67 | 6.48 | 5.05 |
| **IXC** | | | | | 71.10 | 6.47 | 5.06 | 70.79 | 6.48 | 5.05 |
| **XC** | | | | | 70.02 | 5.88 | 5.44 | 69.77 | 5.80 | 5.40 |

[a] Polydispersity index, $M_w/M_n$. [b] Degree of polymerization.

from the low-temperature polycondensation of *N*,*N*′-bis-(trimethylsilyl)-*N*,*N*′-dimethylalkylenediamines with TBOC by Scheme 2b had the highest molecular weights as indicated by their inherent viscosities. The use of N-silylated diamines had several advantages.[27] Silyl-substituted diamines could generally be distilled to yield monomers of high purity. Also, in a typical polycondensation between a diamine and a diacid chloride, an external base is necessary to neutralize liberated hydrochloric acid, but the reaction between a diacid chloride and a *N*,*N*′-silyl-substituted diamine forms a halosilane, which is a nonreactive byproduct.

The yields, physical properties, and $^1$H-NMR chemical shifts for the disilyl derivatives of the various *N*,*N*′-dimethylalkylenediamines are summarized in Tables 1 and 2. The disilyl-substituted N-methylated diamines **3a**−**c** could be readily purified by distillation. Because of the poor solubility of TBOC, the polymerization reactions were initially carried out at temperatures which would afford dissolution, although the polymers prepared with trimethylsilyl-substituted derivatives had the highest molecular weights and the best yields, especially at low temperatures.

In the case of Scheme 2b with silylated amines, as the polymerization proceeded, TBOC very slowly dissolved in the polymerization medium as it reacted with the appropriate silyl-substituted monomer to form polymer. After 4−6 h, TBOC was totally dissolved to yield a viscous polymer solution. Polymers **IC**−**XC** were soluble in 1,1,2,2-tetrachloroethane at a concentration of approximately 1.0 g per 2 mL of solvent, and halogenated solvents were excellent solvents for these polymeric materials. A summary of the reaction conditions, polymerization yields, and solution viscosities for all the polymers prepared is shown in Table 3.

As shown in Table 4, polymers having the highest molecular weight were obtained from the low-temperature solution condensation method using the disilyl-substituted derivatives, **3a**−**c**. For the polymers prepared by Scheme 2b, a very high degree of polymerization was observed indicating the lack of side reactions at low temperatures. A direct relationship was observed between the degree of polymerization and the agreement between the calculated and observed elemental analyses; the highest molecular weight polymers, **VIIIC**−**XC**, showed good agreement but the lowest molecular weight polymer, **IVB**, showed a greater discrepancy.

**Polymer Characterization by NMR Spectroscopy.** Detailed characterization of the possible conformations of the polymers in solution and in the solid state was made possible from the information obtained from the investigation of the model compound, **M**, using NMR spectroscopy. The $^1$H-NMR spectrum of the model compound, shown in Figure 1, revealed the types of conformations which were present both in solution and in the solid state for the polymers prepared. The model compound, **M**, may have both *syn* and *anti* rotational conformers.

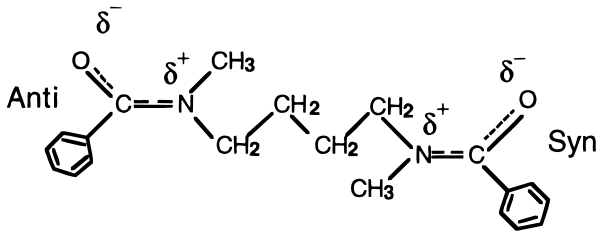


(M)

As shown in Figure 1A, three singlets were observed for the *N*-methyl groups of the model compound in an approximate ratio of 1:2:1. Three broad singlets, which correspond to the methylene groups located in the

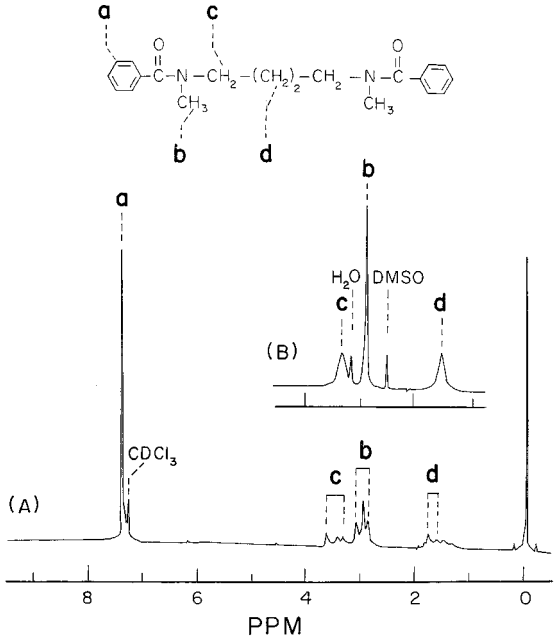


**Figure 1.** $^1$H-NMR spectra of the model compound *N*,*N*′-bis-(benzoyl)-*N*,*N*′-dimethylbutanediamine: (A) in $CDCl_3$, room temperature; (B) in DMSO, 80 °C.

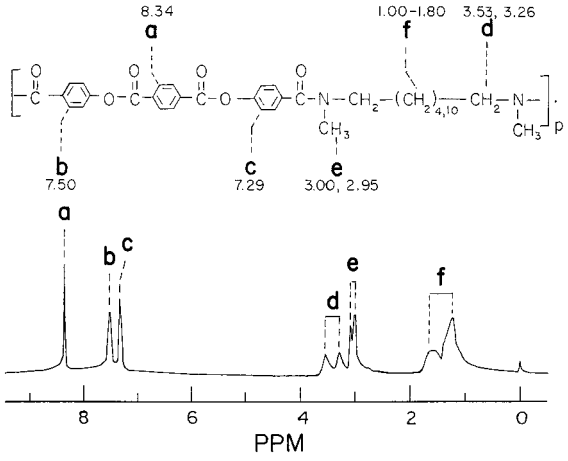


**Figure 2.** $^1$H-NMR spectrum of polymer **VIIIC** in $CDCl_3$, room temperature.

α-position to the nitrogen atom, were also observed. These signals can be assigned to the two rotational isomeric forms of an amide linkage, the *syn* (s) or the *anti* (a) state. Because the model compound contained two amide linkages separated by four methylene units, the following isomers are possible: s:s′, s:a′, a:s′, and a:a′, but the s:a′ state and the a:s′ state are identical. If the *syn* and *anti* isomers were thermodynamically equivalent at room temperature, the peak intensities would be expected to occur in the following ratios 1:2:1 (s:s′, s:a′ = a:s′, a:a′), which was approximately observed. Three possible isomeric states were also shown to occur for *N*,*N*′-dibenzoyl-*N*,*N*′-dimethylethylenediamine.[41] As shown in Figure 1B, when the model compound was heated to 80 °C, broad singlet signals were observed reflecting an averaging of the possible magnetic environments.

When the amide linkages were separated by six methylene units, as was the case with the intermediate **1a** and copolymer **VIIIC**, only a pair of peaks was observed for the methyl groups and the methylene groups. Figure 2 shows the $^1$H-NMR spectrum of copolymer **VIIIC**, with longer flexible spacer units, and

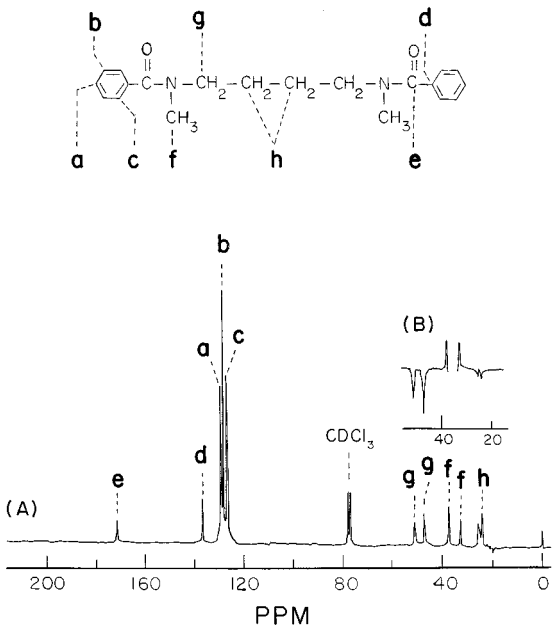


**Figure 3.** $^{13}$C-NMR spectra of the model compound *N*,*N*′-bis-(benzoyl)-*N*,*N*′-dimethylbutanediamine ($CDCl_3$, room temperature): (A) $^{13}$C-NMR spectrum; (B) $^{13}$C-NMR spectrum using the DEPT pulse sequence with no spectrum editing, where $\theta = 135$ °C.

for which the *syn* and *anti* rotational conformers could be clearly observed as sharp doublets.

Further support for the existence of *syn* and *anti* rotational isomers was found in the $^{13}$C-NMR spectrum of the model compound **M**. As shown in Figure 3, the aliphatic region of the spectrum was complex and could not be readily assigned without a multipulse NMR experiment. The spectrum shown in Figure 3B was obtained using the DEPT pulse sequence.[52] With a final $\theta$ pulse of 135 °C, the methyl groups having the *syn* and *anti* conformations could be readily identified at 32.7 and 37.4 ppm, respectively, while the methylene carbons located in the α-position to the nitrogen atom were observed at 46.7 and 50.9 ppm, with the carbon atoms adjacent to the amide functionalities having the *anti* conformation occurring slightly downfield. Unlike the $^1$H-NMR spectrum for the model compound, only *syn* or *anti* conformations were observed for the $^{13}$C spectrum, indicating that the two amide groups were far enough removed that the anisotropy of one amide linkage did not significantly influence the chemical shift of the other.

As shown in Figure 4A for polymer **IXC**, *syn* and *anti* rotational isomers were also readily observed in the $^{13}$C spectrum of the polymers. Using the DEPT pulse sequence, as shown in Figure 4B, the *N*-methyl *syn* and *anti* carbon atoms could be readily identified at 32.8 and 37.6 ppm, respectively. The molecular anisotropy of the carbonyl group was directly observed in the carbonyl region of polymer **IXC**. The amide carbonyl carbon appeared as a doublet at 170.9 and 170.3 ppm, indicating the presence of the *syn* and *anti* groups, which appeared with nearly equal intensity. Assignment of the aromatic carbon atoms was consistent with the assignments previously reported for poly[tetramethyleneterephthaloyl bis(4-oxybenzoate)].[39]

The $^1$H-NMR and $^{13}$C-NMR spectra of the model compound and the corresponding polymers showed the possible conformations which occurred for the polymers in solution. Additional objectives of this study were to investigate the presence of these rotational isomers in

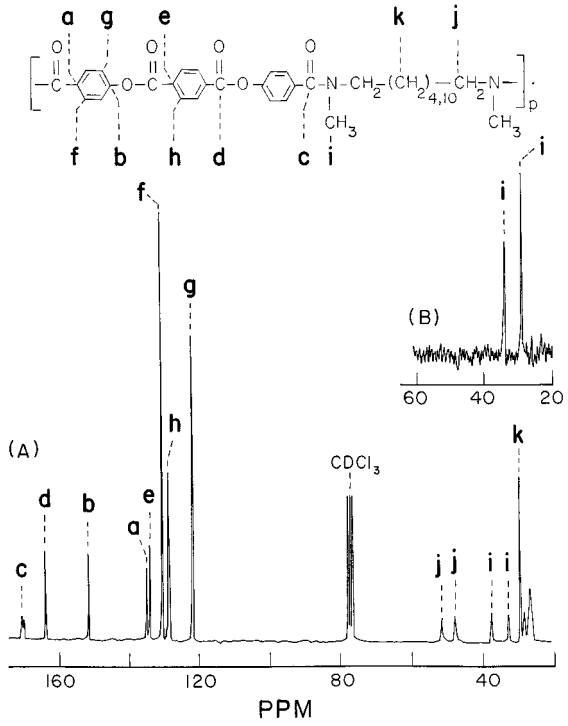


**Figure 4.** (A) $^{13}$C-NMR spectra of polymer **IXC** in $CDCl_3$, room temperature. (B) $^{13}$C-NMR spectrum of polymer **IXC** obtained using the DEPT pulse sequence with spectrum editing to reveal the methyl carbon atoms, where $\theta = 135$ °C, room temperature.

the solid state, to analyze the change in conformation of the polymer in the solid state with increasing temperature, and to attempt to correlate the dependence of polymer conformation on temperature with the liquid-crystalline properties of these polymers.

The dependence of the $^{13}$C-NMR CP/MAS spectrum of polymer **IVB** with temperature is shown in Figure 5. This polymer was precipitated from solution and, thus, had no prior thermal history. As shown by the room temperature spectrum, Figure 5A, the spectrum is consistent with the $^{13}$C-NMR solution spectrum of polymer **IX**. Of particular interest is the pair of peaks which were observed at approximately 50 ppm, which corresponded to the methylene group located α to the amide group. The presence of two peaks indicates that the polymer also consisted of *syn* and *anti* rotational conformers in the solid state. Upon heating to 125 °C, the spectrum sharpened but did not significantly change. The direct evidence of conformational changes was observed upon heating to 185 °C, where the downfield peak assignable to the methylene group located α to the amide group in the *anti* conformation underwent a significant reduction in intensity, as shown in Figure 5C. Also of interest is the region between 30 and 35 ppm containing the linear aliphatic methylene units in the flexible spacer linkage which may include both the *trans* and *gauche* conformations. At both room temperature and at 125 °C, the fraction of *trans* and *gauche* conformations occurred with almost equal intensity. However, at 185 °C there appeared to be an almost complete loss in the intensity of the *trans* conformations.

At 185 °C there was also an apparent loss of intensity of the nonprotonated aromatic and carbonyl carbons which can be explained by the increased molecular motion of the hard segment, including the ring flipping of the aromatic units. As shown in Figure 5D, heating the polymer to 245 °C, a temperature at which the

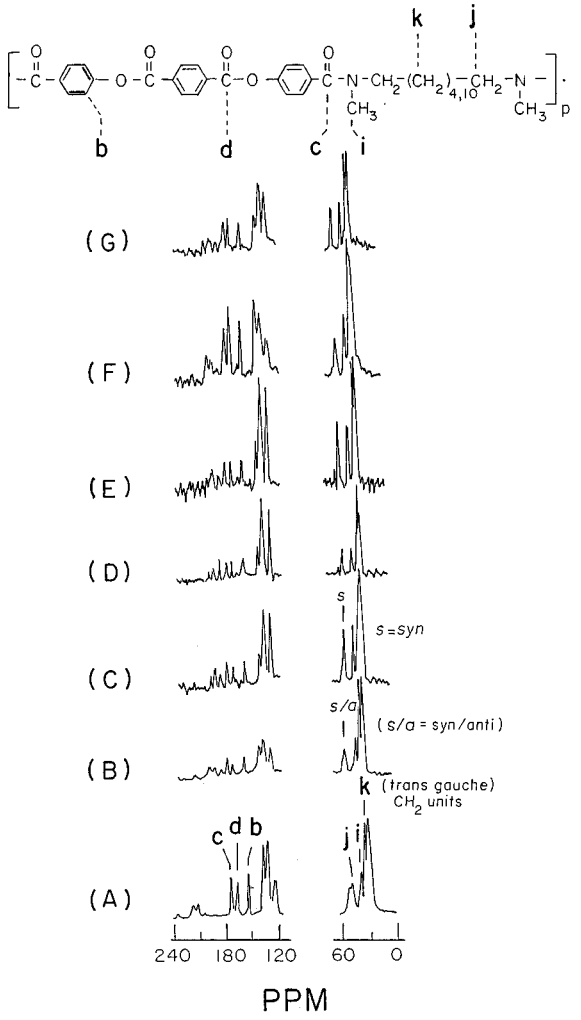


**Figure 5.** $^{13}$C-NMR CP/MAS spectra of polymer **IVB**: (A) room temperature, no thermal history; (B) 125 °C, first heating; (C) 185 °C; (D) 245 °C, melting; (E) 200 °C, first cooling; (F) 30 °C; (G) 125 °C, second heating.

polymer exists in the liquid crystalline molten state, yielded a spectrum containing sharp peaks consistent with extensive molecular motion. The amide groups consisted predominantly of *syn* units while the aliphatic region appeared to be consistent with an average of *trans* and *gauche* conformations. On cooling to 200 °C, as shown in Figure 5E, the amide units retained the *syn* conformation, while considerable molecular motion of the aromatic units was observed. Further cooling of the polymer to room temperature, as shown in Figure 5F, indicated that the amide units consisted exclusively of *syn* units. An increase in intensity of the nonprotonated aromatic and carbonyl units was also observed, suggesting that little molecular motion of the hard segment occurred at this temperature. Subsequent heating to 125 °C, as shown in Figure 5G, did not show any change in polymer conformation relative to room temperature.

From the results of these experiments, the following conclusions can be made. Upon precipitation of the polymer from solution following polymerization, the polymer contained both *syn* and *anti* amide units, while the aliphatic region consisted of almost equal fractions of *trans* and *gauche* methylene units. When the polymer was heated to a temperature between 125 and 185 °C, considerable molecular motion of the polymer chain was observed and amide units having only the *syn* conformation were obtained. After the loss of the *anti*

**Table 5. Thermal Properties of LC Poly(ester amide)s[a]**

| | | 1st melting endotherms | | | 1st cooling exotherms | | | 2nd melting endotherms | | | 2nd cooling exotherms | | |
|---|---|---|---|---|---|---|---|---|---|---|---|---|---|
| polymer | *n* | °C | $\Delta H_m$[b] | $\Delta S_m$[c] | °C | $\Delta H_c$ | $\Delta S_c$ | °C | $\Delta H_m$ | $\Delta S_m$ | °C | $\Delta H_c$ | $\Delta S_c$ |
| **IB** | 12 | 179 | 10.5 | 23.2 | 178 | −12.9 | −28.6 | 147 | 2.7 | 6.4 | 174 | −6.0 | −13.4 |
| | | 234 | 25.5 | 50.3 | | | | 200 | 13.4 | 28.3 | | | |
| **IIB** | 10 | 246 | 22.8 | 43.9 | 175 | −4.4 | −9.8 | 218 | 5.2 | 10.6 | 171 | −1.4 | −3.15 |
| **IIIB** | 12, 6 3:1 | 163 230 | 2.9 21.3 | 6.7 42.3 | 177 | −3.4 | −7.6 | 212 | 8.0 | 16.5 | | | |
| **IVB** | 12, 6 1:1 | 154 223 | 2.3 12.5 | 5.4 25.2 | 171 | −4.4 | −9.9 | 217 | 8.3 | 16.9 | 177 | −1.8 | −4.0 |
| **VB** | 12, 6 1:3 | 274 | 22.0 | 40.2 | 200 | −1.6 | −3.4 | 255 | 10.6 | 20.1 | | | |
| **VIB** | 6 | 293 | 20.5 | 36.2 | | | | 258 | 12.0 | 22.6 | | | |
| **VIIC** | 6 | 302 | 21.3 | 37.0 | 249 | −14.3 | −27.4 | 286 [282 | 11.6 5.61 | 20.8 10.1][d] | 233 [247 | −3.8 −1.0 | −7.51 −1.9][d] |
| **VIIIC** | 12, 6 ∼ 1:1 | 150 260 | 4.6 12.1 | 10.9 22.7 | 213 | −8.8 | −18.1 | 244 | 11.2 | 21.7 | 208 | −9.1 | −18.9 |
| **IXC** | 12, 6 ∼ 1:1 | 144 258 | 2.93 19.6 | 7.0 36.9 | 214 252[e] | −8.9 | 18.3 | 250 [244 | 13.7 10.1 | 26.3 19.6][d] | 207 251[e] [202 264[e]][d] | −7.9 −6.2 | −16.5 −13.1 |
| **XC** | 6 | 308 | 28.3 | 48.7 | 271 294 | −12.9 −1.9 | −23.7 −3.35 | 298 | 20.8 | 36.4 | 260 301 | −12.0 −0.7 | −22.5 −1.2 |

[a] 10 °C/min heating and cooling rate. [b] kJ/mol. [c] J/(mol K). [d] Third heating and cooling. [e] A weak exotherm which appears as a shoulder.

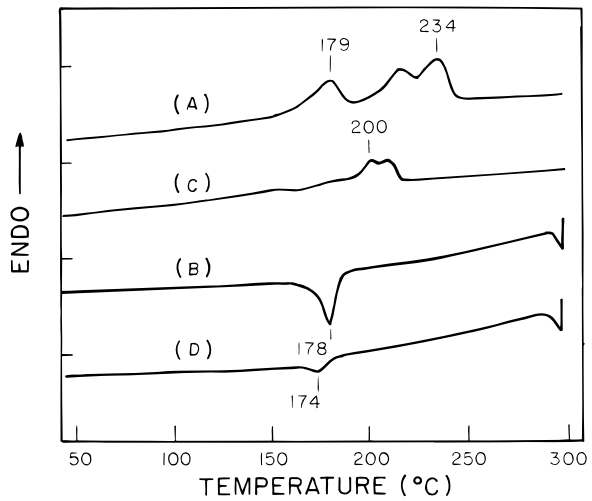


**Figure 6.** DSC thermogram of polymer **IB**: (A) first heating cycle; (B) first cooling cycle; (C) second heating cycle; (D) second cooling cycle.

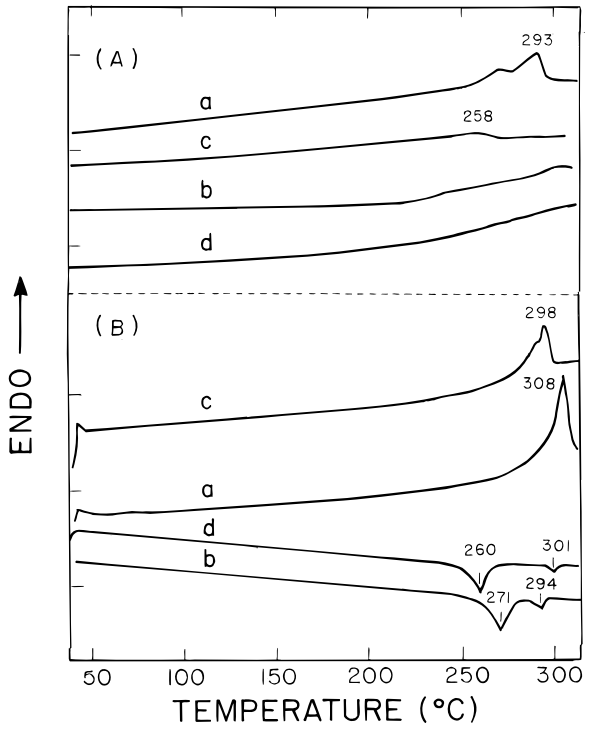


**Figure 7.** (A) DSC thermogram of polymer **VIB**: (a) first heating cycle; (b) first cooling cycle; (c) second heating cycle; (d) second cooling cycle. (B) DSC thermogram of polymer **XC**: (a) first heating cycle; (b) first cooling cycle; (c) second heating cycle; (d) second cooling cycle.

conformation, the *syn* conformation was retained during further heating and cooling cycles, suggesting that the *syn* conformation was the most stable thermodynamic state and is the principal conformation in the mesophase.

**Polymer Thermal Analysis.** The poly(ester amide)s prepared in this investigation were studied by thermogravimetric analysis, TGA, under nitrogen, and exhibited approximately 1% weight loss when heated to 350 °C. In air, however, the poly(ester amide)s had a lower thermal stability. Polymer **VIIC**, for example, showed a 1% weight loss when heated to 263 °C and a 2.5% weight loss at 329 °C.

Analyses of the various polymers by differential scanning calorimetry (DSC) showed that the thermal transitions varied greatly with molecular weight and with flexible spacer chain length. Data from the characterization of the LC poly(ester amide)s by DSC are summarized in Table 5. The DSC heating and cooling scans for polymers **IB**, **IVB**, **VIB**, **VIIIC**, and **XC** are shown in Figures 6, 7, and 8. One noteworthy observation is the endothermic transition which occurred between 150 and 180 °C during the first heating cycle of all polymers containing the 12-methylene flexible spacer unit. The transition occurred over a temperature range in which the polymer had considerable molecular motion, including the flipping of the aromatic segments, the conversion of *anti* amide units to *syn* amide units, as well as a shift in the content of *trans* and *gauche* methylene units in the flexible spacer group, as discussed previously. As seen in Figures 6 and 7, polymer **IB** was the only polymer to show this endotherm both during the first and second heating, but no analogous endotherm was observed prior to polymer melting for any of the LC polymers containing only the shorter six-methylene spacer group (**VIB**, **VIIC**, **XC**).

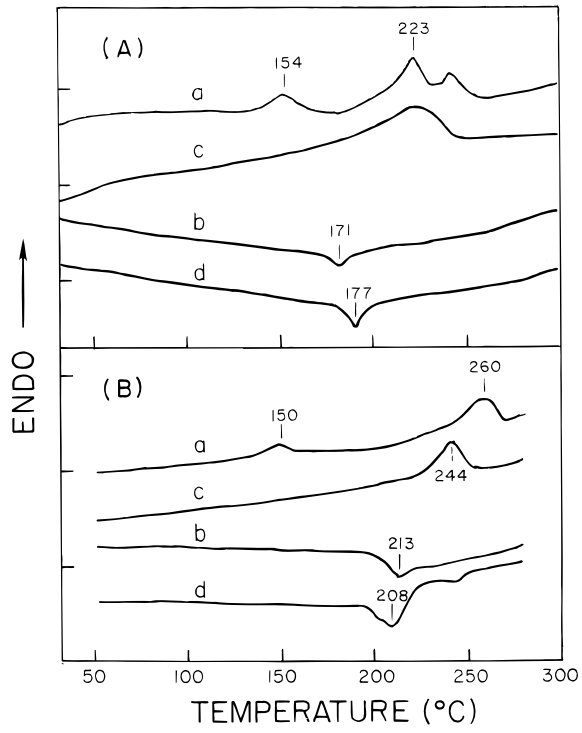


**Figure 8.** (A) DSC thermogram of polymer **IVB**: (a) first heating cycle; (b) first cooling cycle; (c) second heating cycle; (d) second cooling cycle. (B) DSC thermogram of polymer **VIIIC**: (a) first heating cycle; (b) first cooling cycle; (c) second heating cycle; (d) second cooling cycle.

The endotherm occurred at a temperature at which the polymer was capable of considerable molecular motion, but the exact nature of this transition, and its dependence on the flexible spacer chain length, would require additional study. In a related study in which polyesters based on $\alpha,\omega$-bis(4-hydroxybenzoyloxy)alkanes and terephthalic acid were investigated, it was observed that similar endotherms occurred prior to the crystal−liquid crystal transition, and the endotherms were attributed to crystal−crystal phase changes, which might involve reorganization of various polymorphic forms on heating.[53]

The first melting transitions of the polymers varied greatly with flexible chain length, composition, and molecular weight. The principal melting endotherm in the first DSC heating cycle may be attributed to the melting of the crystalline state obtained from solvent-induced crystallization. As shown in Table 5, the first melting transition increased from 293 °C for the lowest viscosity polymer containing a 6-methylene spacer unit (**VIB**) to 308 °C for the highest viscosity polymer having the same composition (**XC**). For the copolymers, the melting points increased with increasing content of the 6-methylene spacer. The effect of molecular weight on polymer melting temperature was greater for copolymers containing mixtures of 6- and 12-methylene spacer units. The principal melting transition for the lowest viscosity copolymer containing a 1:1 ratio of 6- and 12-methylene spacer units occurred at 223 °C, while the highest molecular weight copolymer, **IXC**, melted at 258 °C.

The first DSC cooling cycle and subsequent heating and cooling cycles were difficult to interpret. The DSC thermograms for polymers **VIB** and **XC**, which had the same chemical composition but different molecular weights, are shown in Figure 7. The thermogram of polymer **VIB**, which has a six-methylene spacer unit with the lower inherent viscosity (0.31 dL/g), did not show a distinct exotherm during the first cooling cycle. In contrast, the first cooling thermogram of polymer **XC**, with the same composition as **VIB** and **VIIC** but the highest inherent viscosity (0.88 dL/g), showed a weak exotherm at 294 °C followed by a much larger exotherm at 271 °C. The transitions observed at 301 and 294 °C during the first and second DSC cooling cycles, respectively, for polymer **XC** represent the transition from the isotropic state to the liquid crystalline state, as observed by POM. Polymer **VIB** underwent a direct transition from the solid state to the liquid crystalline state during the first polymer melting transition and did not show a distinct recrystallization exotherm upon subsequent cooling. Polymer **VIB** would be expected to crystallize more readily than polymer **XC** because of its lower melt viscosity. The exotherms observed at 260 and 271 °C during the first and second cooling cycles of polymer **XC** are not well understood because no discernible changes in the liquid crystalline texture of the polymer were observed by POM over this temperature range.

The thermograms of copolymers containing an equal molar ratio of 6- and 12-methylene spacer units, **IVB**, and **VIIIC** and **IXC**, also showed similar behavior with increasing molecular weight, as shown in Figure 8. The thermogram of the polymer having the lowest inherent viscosity, polymer **IVB** (0.38 dL/g), showed a weak exotherm at 171 °C upon cooling which corresponded to a change in enthalpy of −4.4 kJ/mol. Copolymers **VIIIC** and **IXC** which had inherent viscosities of 1.23 and 1.61 dL/g, respectively, had thermograms which showed changes in enthalpy of approximately −8.9 kJ/mol for the principal exotherms.

The cooling cycle thermograms of polymers **VIIIC** and **IXC** also contained a shoulder prior to the primary exotherm, which occurred at 250 °C for both polymers, although the transition was not as sharp as the exothermic peak observed at 301 °C during the first cooling for polymer **XC**. The appearance of the shoulders on cooling of polymers **VIIIC** and **IXC** occurred at temperatures where the liquid crystalline state developed, as observed by POM. The principal exotherms which occurred during the cooling cycles of all the poly(ester amide)s and the weak exotherms which appeared at higher temperature cannot be entirely explained. Because the thermal transitions occurred at increasingly lower temperature and with increasingly smaller changes in enthalpy and entropy with each successive DSC heating cycle, molecular rearrangement may have occurred yielding polymers having different chemical structures. Characterization of the polymers by X-ray diffraction, which will be presented below, shows that the polymers did not appear to crystallize upon cooling and that the polymers formed a disordered solid, which will be referred to as a frozen nematic state. Unlike the first DSC heating thermograms, the principal endotherm of the various copolymers showed a different dependence on copolymer composition during the second DSC heating cycles. The melting temperatures of the various low-viscosity copolymers, **IIIB**, **IVB**, and **VB**, increased with increasing content of the six-methylene spacer.

**Polymer Characterization by Wide Angle X-ray Diffraction, WAXD.** Because many of the polymers were prepared in relatively high molecular weight, it was possible to melt-spin the poly(ester amide)s, PEAs, in the liquid-crystalline state to obtain highly oriented fibers having well-defined X-ray diffraction patterns.

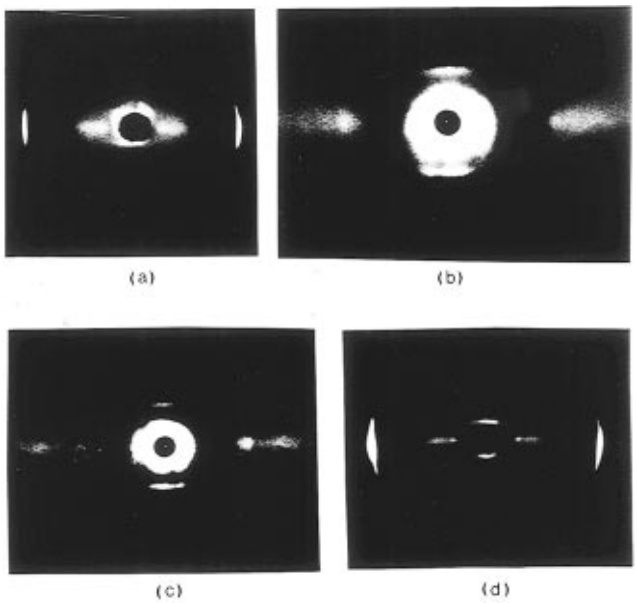


**Figure 9.** Wide angle X-ray diffraction patterns of **PEA-VIIIC** as an oriented melt-extruded fiber (sample-to-film distances were 49.64 mm, weak exposure (w), and 168.78 mm, strong exposure (s)): (a) room temperature, w; (b) room temperature, s; (c) 120 °C, s; (d) 138 °C, w.

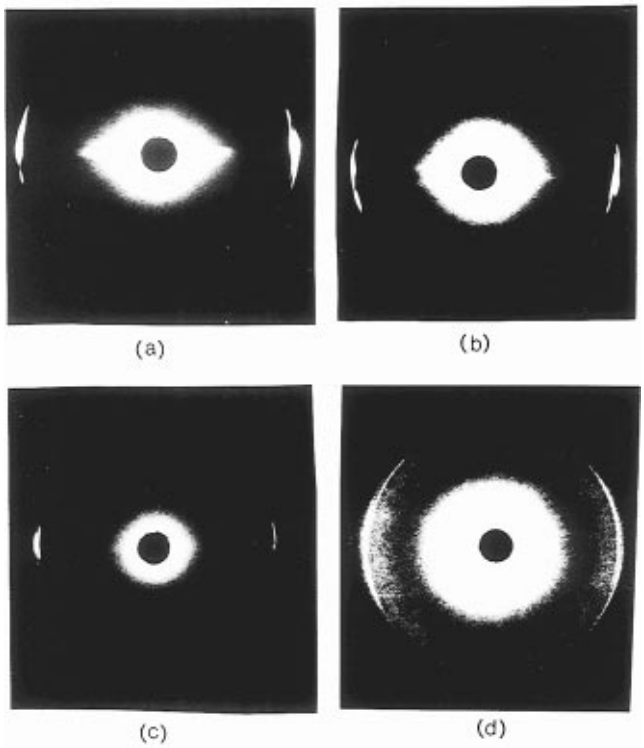


**Figure 10.** WAXD patterns of **PEA-VIIIC** as an oriented melt-extruded fiber (sample-to-film distance was 49.64 mm: (a) 180 °C; (b) 218 °C; (c) 238 °C; (d) fiber heated directly from room temperature to 240 °C without exposures at intermediate temperatures.

Figures 9 and 10 show the WAXD patterns of **PEA-VIIIC** taken at increasing temperatures. The reflections for all samples are summarized in Table 6. The WAXD patterns can be described as those of a nematic organization with local preferred azimuthal orientation. The fiber direction for the WAXD shown in Figures 9 and 10 is vertical.

The WAXD pattern of **PEA-VIIIC** at room temperature is characterized by two arcs located on the equator which correspond to an interchain distance of 4.45 Å. The reflections are sharp indicating that the spacings between the parallel aligned chains were regular. Parts b and c of Figure 9 show the WAXD patterns in which the reflections at the lower angles appear more clearly. Two diffuse streaks can be observed along the equator. These types of reflections have been previously observed in highly ordered nematic liquid crystals, and although the source of the reflections is unknown, they have been attributed to voids.[54] Reflections were also observed along the meridian which can be attributed to the short range order of the repeat units along the polymer backbone.

The WAXD patterns in parts a−c of Figure 10 show that the liquid crystalline order present at room temperature changed significantly at higher temperatures. At 180 °C the reflections which occurred at the lower temperatures along the meridian became diffuse, suggesting that a loss in short range periodicity occurred along the polymer backbone. Reflections along the meridian corresponding to the periodic distance of the repeat units along the polymer backbone were barely detectable when a longer sample-to-film distance of 168.78 mm was used. At higher temperatures, no reflections were discerned from the diffuse halo which appeared at temperatures exceeding 180 °C, even when a longer sample-to-film distance was used, suggesting a complete loss of order along the polymer backbone. However, the reflections along the equator, which correspond to the distance between the chains, became progressively sharper.

At 238 °C, the arcs along the equator became very sharp indicating that the distance and the degree of packing between the chains were very uniform. However, the periodicity along the polymer backbone successively diminished, until at 180 °C it could no longer be observed, indicating that the highly ordered nematic texture obtained from melt-spinning was lost at high temperature to form a less ordered nematic state.

Figure 10d shows a WAXD pattern of a **PEA-VIIIC** fiber sample which was heated directly from room temperature to 240 °C without exposure to intermediate temperatures. This diffraction pattern also shows nematic order, with no periodicity along the polymer backbone but significant order between the chains, although the degree of organization between the chains was less than that present in the previously described fiber samples. The fact that the otherwise sharp arcs along the equator developed into an outer ring indicates the loss of orientation in the fiber which occurred when the fibers were heated directly to their melting point, suggesting that many LC domains developed which were tilted with respect to each other.

The changes which occurred in the WAXD pattern of the powder sample polymer **IVB** illustrate the complexity of the thermal transitions of these PEAs. Figure 11 shows the dependence of X-ray intensity with 1/*d* (Å) for various temperatures. Figure 11a shows the X-ray intensity of the sample obtained from solvent precipitation with no thermal heat treatment. This curve shows multiple reflections indicative of the crystalline state. During the first DSC heating cycle shown in Figure 8a, polymer **IVB** had an endotherm at 154 °C with an enthalpy change of 12.5 kJ/mol. Polymer **IVB** was heated to 175 °C and exposed to X-rays for 2.5 h. The X-ray intensity dependence as a function of 1/*d* (Å) is shown in Figure 11b. However, no observable change in the intensity distribution obtained at 175 °C relative

**Table 6. WAXD Reflections for Poly(ester amide)s at Various Temperatures**

| | | | | LC state[a] | | |
|---|---|---|---|---|---|---|
| polymer | form[b] | temp (°C) | crystalline reflections[a] | $d^c$ (Å) | $D^d$ (Å) | other (Å) |
| **IVB** | P | RT[e] | 3.18 (w,s); 3.96, 4.34 (s); 4.69 (s); 7.58 (w,d); 16.2 (s,d) | | | |
| **IVB** | P | 180 | 3.18 (w,s); 4.05, 4.42 (s); 4.69 (s); 8.38 (w,d); 16.2 (s,d) | | | |
| **IVB** | M | 250 | | 4.51(d) | 9.10−23.59 (d) | |
| **IVB** | S | RT | | 4.51 (s) | | |
| **VIIC** | F | RT | | 4.51 (s) | 28.04 (m) (27.1)[f] | 5.97 (s,w) |
| **VIIIC** | F | RT | | 4.45 (s) | 30.64 (s) (27.1−33.5)[g] | |

[a] w = weak intensity; s = strong intensity; d = diffuse; m = moderate intensity. [b] P = powder sample; F = fiber sample; M = molten sample; S = solid obtained after slow cooling from the melt. [c] Equatorial layer spacing between adjacent mesogenic units. [d] Meridional layer spacing associated with the length of the polymer repeat unit. [e] Room temperature. [f] Calculated layer spacing assuming an all *trans* conformation for the six-methylene flexible spacer unit. [g] Calculated layer spacing assuming an all *trans* conformation having from 6- to 12-methylene flexible spacer units.

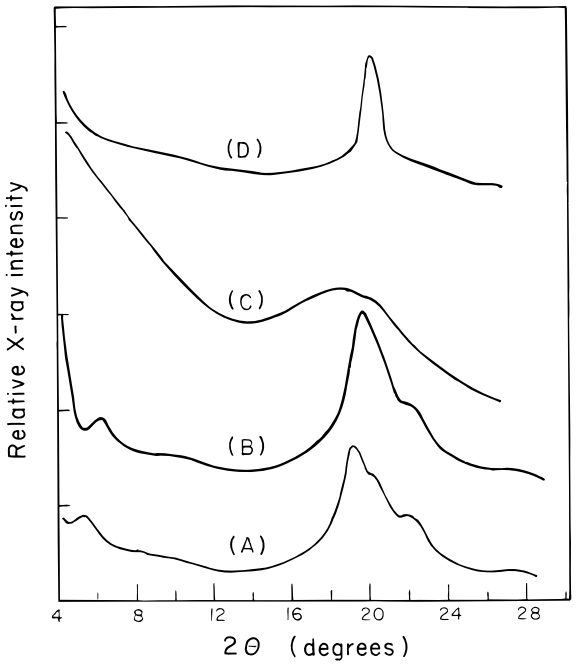


**Figure 11.** Dependence of X-ray intensity with 1/*d* (Å) for polymer IVB at various temperatures: (A) room temperature; (B) 180 °C; (C) 250 °C; (D) sample heated to 280 °C and cooled to room temperature at approximately 10 °C/min.

to room temperature was observed. In a related study of poly[tetramethylene terephthaloyl bis(4-oxybenzoate)], it was shown by X-ray diffraction that prior to polymer melting, an irreversible crystal−crystal phase transition occurred involving the conformation of the flexible spacer units and the orientation of the aromatic rings.[39]

When polymer **IVB** was heated to and held at 250 °C, a temperature slightly higher than the crystalline melting transition, a diffuse outer halo was observed, indicating a lower degree of order between the chains, as well as a diffuse inner halo at the lower angles which suggested a random displacement of the repeat units along the polymer backbone. This WAXD behavior is consistent with that of a nematic liquid-crystalline phase. The dependence of X-ray intensity with 1/*d* (Å) at 250 °C is shown in Figure 11c. However, because polymer **IVB** was heated at 250 °C for a prolonged time period, the diffuse reflections may be attributed to an irregular polymer structure resulting from molecular interchange reactions; thus the conclusions should be considered tentative.

Polymer **IVB** was also melted at 280 °C in a sealed glass capillary on a Fisher-Johns melting point apparatus and slowly cooled to room temperature at a rate of approximately 10 °C/min. The polymer did not appear to crystallize upon cooling from the melt, as shown by the dependence of X-ray intensity with 1/*d* (Å) in Figure 11d. As shown in Table 6, the reflection having the highest intensity in the crystalline state for polymer **IVB** was at 4.69 Å. The only reflection which was observed for polymer **IVB** after the previously described heat treatment was a sharp reflection occurring at 4.51 Å. Although solidification occurred, X-ray diffraction indicated that the polymer did not appear to have crystallized, a phenomenon previously observed for a related polyester having lateral methyl units, poly-[oxy(1,4-dimethyltetramethylene)oxycarbonyl-1,4-phenyleneoxyterephthaloyloxy-1,4-phenylenecarbonyl].[26] In this case, a solid was obtained which had a degree of order resembling that of parallel spaced chains having random sequences along the polymer backbone.

Fiber sample **PEA-VIIC** was observed by X-ray diffraction 13 months after the initial melt-extrusion and showed no reflections indicative of polymer crystallization. The X-ray diffraction pattern of sample fiber **PEA-VIIC** had a pair of arcs along the equator, which corresponded to a *d*-spacing of 4.51 Å, and low angle reflections along the meridian, which were difficult to distinguish from a diffuse halo. The meridional reflections corresponded to a *d*-spacing of 28.04 Å. At higher angle there were two additional reflections along the meridian which were relatively weak and corresponded to a *d*-spacing of 5.97 Å.

The observed layer spacings for fibers obtained from polymers **VIIC** and **VIIIC** showed good agreement with the calculated layer spacings, as shown in Table 6. The calculated layer spacing assumes an all *trans* conformation for the polymethylene flexible spacer units, and an amide linkage in which the attached phenyl group was located *cis* to the methyl group and *trans* to the methylene unit. A C−N bond having appreciable double bond character would have a longer theoretical repeat unit and may explain why the observed layer spacings are slightly greater than the calculated values.

**Polymer Characterization by Polarized Optical Microscopy, POM.** Observation of the poly(ester amide)s by POM revealed the complex nature of their transitions. After polymer **XC** was melted on a hot-stage between cover slides and observed under cross-polarizers at 315 °C, only a dark isotropic texture was seen. As shown by the DSC scan in Figure 7B, the polymer exhibited a weak exotherm at 301 °C during the cooling cycle. As the sample was cooled to below 301 °C a dense nematic schlieren texture developed. Hence, the polymer showed monotropic behavior with formation of the LC phase below the melting temperature of the crystalline state.

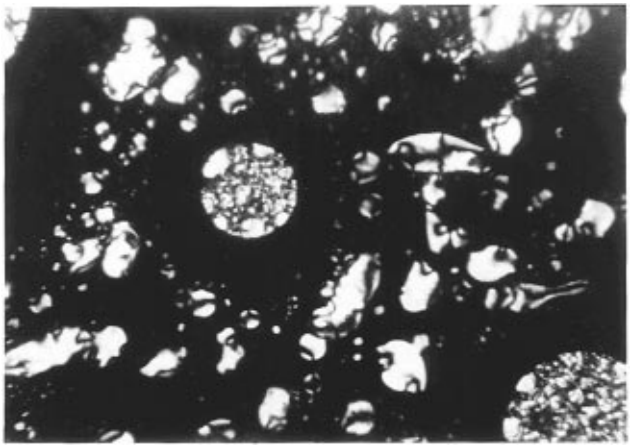

**Figure 12.** Polymer **XC** at 280 °C observed by polarizing optical microscopy (magnification equals 400×) (Figure was reduced 50% for publication.)

If the melt of PEA-XC was sheared at 280 °C, a brilliantly birefringent texture developed, as shown in Figure 12, and after annealing the sample for 1 h at 280 °C, a well-defined threaded nematic schlieren texture was formed. On subsequent cooling to 250 °C, a temperature below the exotherms observed at 271 °C for the first DSC cooling cycle and 260 °C for the second cooling cycle of polymer **XC**, no change occurred in the homogeneous threaded nematic texture, even after annealing for 1 h. When the sample was heated again to above 301 °C, the temperature at which an endotherm was observed during the second DSC heating cycle, the texture became highly birefringent and the polymer flowed, although the pattern still appeared to be a nematic schlieren texture. The LC phase was stable up to 350 °C, the limiting temperature of the hot stage used, although dark isotropic regions could be observed. Because melting endotherms and cooling exotherms became progressively weaker with the length of heating, as shown in Table 5, only tentative conclusions can be drawn from annealing studies at these temperatures.

Since the lower molecular weight polymers had thermal transitions which occurred at lower temperatures, annealing studies could be conducted at lower temperatures without significant thermal degradation. When polymer **IVB** was heated to 240 °C, melted between glass slides, and annealed for 1 h, a threaded nematic texture was observed. Upon cooling to approximately 210 °C, the sample solidified and could no longer be sheared. After subsequent heating and annealing at 225 °C for 1 h, the well-defined threaded nematic texture appeared to flow. Upon cooling to 160 °C at 10 °C/min, a temperature below that of the cooling exotherms observed in the first and second DSC cooling cycle of **IVB**, the density of the nematic threads slightly diminished but could clearly be observed. After 1 h of annealing at this temperature, the polymer still showed a threaded nematic texture, although the sample appeared to have solidified and could not be sheared readily. Upon heating to 240 °C, the sample flowed and appeared as a dense threaded nematic texture. After cooling at 10 °C/min to 110 °C and annealing for 15 h, the polymer still appeared to have a threaded nematic texture, although it seemed to be in a solid state.

Because various first-order transitions observed in the DSC thermograms may be associated with conformational changes of the long flexible spacer groups, observations by POM of polymer **IB**, which contained the 12-methylene spacer, were of interest. Polymer **IB** melted at 234 °C to yield a dark isotropic melt which flowed but showed no birefringence, and shearing failed to induce a liquid crystalline texture. Upon cooling from the melt at 10 °C/min, a threaded nematic texture progressively developed until 160 °C, below which the polymer no longer appeared to flow. When the sample was subsequently heated to 225 °C, the intensity of the threaded nematic texture decreased until isotropization occurred at 225 °C. The polymer containing the 12-methylene spacer was the only polymer observed to have an isotropization temperature.

It is well-known that for some LCP polymers shearing enhances the formation of a nematic texture. For hydrogen-bonded polyurethanes, shearing was found necessary to observe typical nematic patterns by POM.[55] For all of the polymers containing the six-methylene spacer unit, shearing induced the formation of the liquid crystalline state directly upon melting. When cooled below the initial melting point, the samples readily formed threaded nematic textures. The transition to a liquid crystalline state was verified by DSC. The thermograms of the higher molecular weight polymers contained either a weak exothermic shoulder or a weak exothermic peak on cooling to a temperature at which the formation of the liquid crystalline state was observed by POM. As the sample was cooled below the lower principal exotherm, solidification occurred, as indicated by both visual inspection and the resistance to shearing. A disordered solid was obtained in which the threaded nematic texture appeared to be frozen. Subsequent annealing at temperatures as low as 100 °C for 15 h formed a texture that appeared as a threaded nematic LC phase. This conclusion was substantiated by X-ray scattering which showed only a single reflection for **PEA-IVB** upon cooling from the melt.

## Conclusions

A series of liquid crystalline poly(ester amide)s were prepared from terephthaloylbis(4-oxybenzoyl chloride) and various *N*,*N*′-dimethylalkylenediamines. The poly(ester amide)s were prepared by three different synthetic methods yielding polymers having a broad distribution of molecular weights. Polymers having the highest molecular weights were prepared from terephthaloylbis(4-oxybenzoyl chloride) and *N*,*N*′-trimethylsilyl-*N*,*N*′-dimethylalkylenediamines.

$^{1}$H- and $^{13}$C-NMR solution spectroscopy showed that these polymers, when precipitated from solution, contained approximately equivalent amounts of *syn* and *anti* amide units. $^{13}$C CP/MAS solid-state NMR spectroscopy revealed that upon heating the polymers into the molten state, the *syn* amide linkage was the most stable thermodynamic state and, once formed, existed to the exclusion of the *anti* form. It was also shown that the polymers were capable of considerable molecular motion at temperatures well below the crystalline melting temperature, which included the rotation of the aromatic units, the interconversion of *trans* and *gauche* methylene units, and the conversion of mixed *syn* and *anti* amide units to exclusively *syn* units.

The formation of the LC phase for the low molecular weight polymers occurred upon initial polymer melting. However, in the absence of shearing, the high molecular weight polymers showed only a dark isotropic texture upon initial melting. After initial melting, the formation of the LC phase for the high molecular weight polymers occurred most readily upon cooling, as shown by POM

and DSC. The poly(ester amide)s were shown by POM and X-ray diffraction to form nematic liquid crystalline phases, although the degree of long and short range order in the nematic phase varied with temperature and sample history. The poly(ester amide) which had the lowest isotropization temperature was the polymer containing the longest flexible 12-methylene spacer linkage. The lower isotropization temperature is attributed to a large increase in entropy upon melting associated with polymers having long flexible spacer units. LCPs containing shorter 6-methylene flexible spacer units exhibited the most birefringent LC textures and, upon formation of the LC state, showed no isotropization temperature below 350 °C. After initial melting, there was no indication of subsequent crystallization for the *N*-methyl substituted poly(ester amide)s. Upon cooling from the LC phase, a disordered solid phase was obtained which appeared to be a frozen nematic state. The polymers seemed to undergo a transition between a frozen nematic LC state and a flowing nematic LC state during subsequent heating and cooling cycles.

**Acknowledgment.** This research was supported by a grant from Akzo Nobel Inc.

## References and Notes

(1) Cowie, J. M.; Wu, H. H. *Br. Polym. J.* **1988**, *20*, 515.
(2) Schmucki, M.; Jenkins, A. D. *Makromol. Chem.* **1989**, *190*, 1303.
(3) Griffin, A. C.; Britt, T. R.; Campbell, G. A. *Mol. Cryst. Liq. Cryst.* **1982**, *82*, 145.
(4) Uryu, T.; Song, J. C. *Polym. J.* **1989**, *21* (12), 977.
(5) Ringsdorf, H.; Tschirner, P. *Makromol. Chem.* **1987**, *188*, 1431.
(6) Aharoni, S. M. *Macromolecules* **1988**, *21*, 1941.
(7) Khan, A. H.; McIntyre J. E.; Milburn, A. H. *Polymer* **1983**, *24*, 1610.
(8) He, Z.; Whitcombe, M. J.; Mitchell, G. R. *Br. Polym. J.* **1990**, *23*, 41.
(9) Uryu, T.; Song, J. C.; Kato, T. *Polym. J.* **1989**, *21* (5), 409.
(10) McIntyre, J.; Milburn, A. H. *Br. Polym. J.* **1981**, March, 5.
(11) Paci, M.; Lupinacci, D.; Bresci, B. *Thermochim. Acta* **1987**, *122*, 181.
(12) Siegmann, A.; Dagan, A.; Kenig, S. *Polymer* **1985**, *26*, 1325.
(13) Chung, T. S. *Plast. Eng.* **1987**, Oct, 39.
(14) La Mantia, F. P.; Valenza, A.; Magagnini, P. L. *Polym. Eng. Sci.* **1990**, *30* (1), 7.
(15) Park, H. S.; Kyu, T. *J. Macromol. Sci., Phys.* **1990**, *B29*, 263.
(16) Kyu, T.; Chen, T. I.; Park, H. S.; White, J. L. *J. Appl. Polym. Sci.* **1989**, *37*, 201.
(17) Weiss, R. A.; Lu, X. *Polym. Prep. (Am. Chem. Soc., Div. Polym. Chem.)* **1992**, *33* (2), 616.
(18) Jin, J.-I.; Antoun, S.; Ober, C.; Lenz, R. W. *Br. Polym. J.* **1980**, Dec, 132.
(19) Ober, C. K.; Jin, J.-I.; Lenz, R. W. *Makromol. Chem., Rapid Commun.* **1983**, *4*, 49.
(20) Ober, C.; Jin, J.-I.; Lenz, R. W. *Polym. J.* **1982**, *14* (1), 9.
(21) Antoun, S.; Lenz, R. W.; Jin, J.-I. *J. Polym. Sci., Polym. Chem. Ed.* **1981**, *19*, 1901.
(22) Bilibin, A. Y.; Ten'kovtsev, A. V.; Piraner, O. N.; Skorokhodov, S. S. *Vysokomol. Soyed*in. **1984**, *A26* (12), 2570.
(23) Bilibin, A. Y.; Ten'kovtsev, A. V.; Skorokhodov, S. S. *Makromol. Chem., Rapid Commun.* **1985**, *6*, 209.
(24) Bilibin, A. Y.; Pashkovsky, E. E.; Ten'kovtsev, A. V.; Skorokhodov, S. S. *Makromol. Chem., Rapid Commun.* **1985**, *6*, 545.
(25) Skorokhodov, S. S.; Bilibin, A. Y. *Makromol. Chem., Macromol. Symp.* **1989**, *26*, 9.
(26) del Pino, J.; Rocha, C. M.; Gomez, M. A.; Fatou, J. G. *Makromol. Chem.* **1992**, *193*, 2251.
(27) Kricheldorf, H. R. *Makromol. Chem., Macromol. Symp.* **1992**, *54/55*, 365.
(28) Imai, Y.; Hamaoka, N.; Kakimoto, M. *J. Polym. Sci., Polym. Chem. Ed.* **1984**, *22*, 1291.
(29) Biggs, B. S.; Frosch, C. J.; Erickson, R. H. *Ind. Eng. Chem.* **1946**, *38* (10), 1016.
(30) Takayanagi, M.; Katayose, T. *J. Polym. Sci., Polym. Chem. Ed.* **1981**, *19*, 1133.
(31) Jadhav, J. Y.; Krigbaum, W. R.; Preston, J. *Macromolecules* **1988**, *21*, 538.
(32) Hatke, W.; Land, H.; Schmidt, H. W. *Makromol. Chem., Rapid Commun.* **1991**, *12*, 233.
(33) Meurisse, P.; Noel, C.; Monnerie, L.; Fayolle, B. *Br. Polym. J.* **1981**, *55*, 13.
(34) Chiellini, E.; Galli, G.; Carrozino, S.; Gallot, B. *Macromolecules* **1990**, *23*, 2106.
(35) Chiellini, E.; Galli, G.; Malanga, C.; Spassky, N. *Polym. Bull. (Berlin)* **1983**, *9*, 336.
(36) Gallot, B.; Galli, G.; Chiellini, E. *Makromol. Chem., Rapid Commun.* **1987**, *8*, 417.
(37) Hatfield, G. R.; Aharoni, S. M. *Macromolecules* **1989**, *22*, 3807.
(38) Frech, C. B.; Adam, A.; Falk, U.; Boeffel, C.; Spiess, H. W. *New Polym. Mater.* **1990**, *2* (3), 267.
(39) del Pino, J.; Gomez, M. A.; Marco, C.; Ellis, G.; Fatou, J. G. *Macromolecules* **1992**, *25*, 4642.
(40) Lyerla, J. R.; Economy, J.; Maresch, G. G.; Muehleback, A.; Yannoni, C. S.; Fyfe, C. A. In *Liquid-Crystalline Polymers*; Weiss, R. A., Ober, C. K., Eds.; ACS Symposium Series 435; American Chemical Society: Washington, DC, 1990; p 359.
(41) Miron, Y.; McGarvey, B. R.; Morawetz, H. *Macromolecules* **1969**, *2* (2), 154.
(42) Kricheldorf, H. R.; Doering, V. *Makromol. Chem.* **1988**, *189*, 1425.
(43) Richards, S. *A. Laboratory Guide to Proton NMR Spectroscopy*; Blackwell Scientific Publications: Cambridge, MA, 1988; p 101.
(44) Morgan, P. W. *Macromolecules* **1977**, *10*, 1381.
(45) Close, L. G., Jr.; Fornes, R. E.; Gilbert, R. D. *J. Polym. Sci.: Polym. Phys. Ed.* **1983**, *21*, 1825.
(46) English, A. D. *J. Polym. Sci.: Polym. Phys. Ed.* **1986**, *24*, 805.
(47) Fritz, H.; Hug, P.; Sauter, H.; Winkler, T.; Logemann, E. *Org. Magn. Reson.* **1977**, *9* (2), 108.
(48) De Vries, A. *Mol. Cryst. Liq. Cryst.* **1985**, *131*, 125.
(49) Azaroff, L. V. *Mol. Cryst. Liq. Cryst.* **1980**, *60*, 76.
(50) Devinsky, F.; Lacko, I.; Krasnjec, L. *Synthesis (Int. J. Methods Synth. Org. Chem. Commun.* **1980**, Apr, 303.
(51) Mc Carthy, T. F.; Lenz, R. W.; Kantor, S. W. *J. Polym. Sci., Polym. Chem. Ed.* **1994**, *32*, 2883
(52) Derome, A. E. *Modern NMR Techniques for Chemistry Research*: Pergamon Press: New York, 1987; pp 143−151.
(53) Frosini, V.; Petris, S. D.; Chiellini, E.; Galli, G.; Lenz, R. W. *Mol. Cryst. Liq. Cryst.* **1983**, *98*, 223.
(54) Noel, C.; Friedrich, C.; Laupretre, F.; Billard, J.; Bozio, L.; Strazielle, C. *Polymer* **1984**, *25*, 263.
(55) Lee, J. B.; Kato, T.; Ujiie, S.; Iimura, K.; Uryu, T. *Macromolecules* **1995**, *28*, 2165.

MA960421U